https://doi.org/10.37965/jdmd.2026.1596

On the Effects of the Overhang Rotor of the Exciter on the Twice per Revolution Vibration of Large two-pole Power Generators

S. Chatterton, A. Vania, L. Dassi, A. Riva, P. Pennacchi*

Politecnico di Milano, Department of Mechanical Engineering, Via Giuseppe La Masa 1, 20156 Milan, Italy

*Corresponding author: paolo.pennacchi@polimi.it

Received 30 June , 2026; Revised 1 September,2026; Accepted 9 November, 2026; Published online 11 November , 2026.

In large two-pole power generators, the anisotropy of the active part of the rotor causes twice per revolution (2X) vibrations whose amplitude depends on the rotational speed. When the speed approaches half the first critical bending speed, the so-called 2X resonance is excited. At such low speeds, the damping provided by oil-film journal bearings is often quite low and 2X vibration levels can become considerable. In generators mounted on only two main supports, a long and slender overhang shaft of the exciter can amplify this phenomenon, as its significant bending enhances the dynamic deflection at the midspan of the rotor. This paper investigates the beneficial effects of installing an additional oil-film journal bearing at the end of the overhang shaft of the exciter. A finite element model of a 600 MVA generator, whose equations of motion have been integrated in the time domain, was used to simulate the 1X and 2X vibrations accounting for the speed-dependent properties of the journal bearings and the periodic variations of the bending stiffness of the shaft. The numerical predictions are validated against experimental vibration data collected during speed transients before and after the installation of the additional support. Both experimental and numerical results demonstrate that the additional bearing significantly reduces the peak of the 2X vibration that occur at the main supports.

Keywords: 2X resonance, generator rotor, overhang shaft, journal bearing, vibration

INTRODUCTION

The slip rings of large generators installed in thermoelectric power plants are commonly mounted on the end part of the shaft located toward the non-drive end (NDE). In many cases, this part of the generator is a slender overhang shaft with a fairly small average diameter, except for the larger diameter of the collector rings, which mainly contributes to the mass of this part of the shaft rather than to its bending stiffness.

Sometimes, the rotor of the generator is only supported on two main journal bearings, even in case of a rather high ratio between length and average diameter of the end part of the shaft where the slip rings are installed.

The overhang shafts of power plant generators are often affected by high vibration levels that may cause an excessive rate of wear of the carbon brushes as they rub against the slip rings. As a result, in order to reduce the amplitude of the lateral vibrations that may affect the slip rings it might be necessary to mount an additional journal bearing downstream the exciter [1].

In large two-pole power generators producing an output frequency of 50 Hz or 60 Hz the first two critical bending speeds are commonly contained in the range of the rotational speed below the rated speed. During runups and coastdowns of the power unit, if the generator rotor is only supported on two main journal bearings, as it passes through these two critical speeds the overhang part of the shaft is often subjected to high vibration levels, even in case of a rather low residual imbalance. This is due to the shape of the flexural eigenmodes related to the first two critical bending speeds of the generator. Indeed, they are characterized

https://doi.org/10.37965/jdmd.2026.1596

by a significant deflection of the overhang shaft on which the slip rings are mounted.

Length and average diameter of this part of the shaft are often contained into pre-established ranges regardless of the size of the power generator. Because of its common geometrical and mechanical parameters, the overhang shaft of the exciter can be characterized by a local flexural normal mode related to a critical speed that is rather close to the rated speed of the power unit. The shape of this normal mode is quite similar to that of the first bending mode of a cantilever beam. If the width of the peak of this resonance is such that it interferes with the rated speed the overhang shaft of the exciter might be affected by noticeable vibration levels in the operating condition. This may accelerate the wear of the carbon brushes that are in contact with the slip rings of the exciter.

The main body of two-pole generator rotors, also denoted the active part of the generator, is characterized by an axial asymmetry. Indeed, the two poles and the multiple slots housing the copper bars cause different values of the principal area moments of inertia of the cross-sections of this part of the rotor [2]. As a result, during a full revolution of the generator the bending stiffness of the shaft evaluated in vertical direction is affected by two periodic variations. This phenomenon causes twice per revolution vibrations (2X) whose amplitude depends on the machine rotational speed [3], [4].

In case of large two-pole generators the slenderness of the rotor is often considerable. Consequently, the low bending stiffness and the considerable mass of the rotor can cause large values of the shaft deflection induced by the weight loading. In addition, the first critical bending speed may be fairly low.

Due to the anisotropy of the main body of the rotor, when the rotational speed reaches half the first critical bending speed the periodic variations of the bending stiffness of the shaft cause double-frequency equivalent forces that excite the first balance resonance of the generator [5]. Therefore, the amplitude of the 2X vibration of the rotor can be significantly amplified. This phenomenon is commonly denoted 2X resonance [6], [7].

When it occurs at a rather low rotational speed the damping forces generated by the oil-film in the journal bearings may be fairly low. In that case, they may be unable to mitigate the amplitude of the 2X vibration, which may reach considerable peak levels both at the midspan between the two supports and at the end of the overhang shaft of the exciter. The level of this 2X vibration can be rather high also at the journal bearings, to the point of approaching the alarm level established by ISO standards [8] or the machine manufacturer.

When the 2X vibration and the corresponding forces excite the first balance resonance, if exciter shaft is not constrained with a further journal bearing, the dynamic deflection of the overhang shaft can enhance the maximum amplitude of the vibrations that occur both at the midspan of the rotor and near the two main journal bearings. In this context, it should be noted that this 2X vibration cannot be mitigated increasing the degree of the shaft balancing as it mainly relates to the anisotropy of the active part of the generator. Indeed, this 2X vibration mainly depends on the difference between the two principal area moments of inertia of the cross-section of the main body of the generator rotor, by the slenderness of the shaft and by the damping properties of the oil-film journal bearings.

Frequently, the first local bending mode that affects the overhang shaft of the exciter is associated with a critical bending speed that is rather close to the nominal speed of the power unit. This resonance can be shifted away from the rated speed installing an additional support downstream of the exciter.

Furthermore, the presence of this additional support also modifies the shape of the first two bending normal modes of the generator rotor, especially in the end part of the shaft located downstream of the exciter. A lower dynamic deflection of this part of the shaft also reduces the maximum magnitude of the bending of the rotor that occurs at the midspan between the two main supports when the first balance resonance is excited. Thanks to this, it is possible to significantly mitigate even the peak level of the 2X vibration measured near the two main journal bearings when the rotational speed reaches half the first critical speed of the generator.

Consequently, installing an additional support at the end of the overhang shaft of the exciter can reduce both the 1X vibration of the slip rings that occur at the rated speed and the 2X vibration of the main body of the generator induced by the excitation of the 2X resonance [9].

Furthermore, the mitigation of the 1X and 2X vibrations also reduces the risk of transverse cracks initiation in some critical parts of the rotor that may be subjected to stress concentrations [10].

This work explains the results gathered by an investigation focused on the dynamic behavior of generator rotors caused by the installation of an additional oil-film journal bearing at the end part of the shaft downstream of the exciter. The numerical results provided by a finite-element model of the rotor system

https://doi.org/10.37965/jdmd.2026.1596

have confirmed the experimental findings collected during speed transients of a large power unit whose generator was originally mounted on only two supports. However, a third support was later installed at the end of the overhang shaft of the exciter.
More in particular, the numerical results pointed out the capability of the additional support to cause a significant mitigation of the relevant levels of the 2X vibration of the generator that occurs when the rotational speed is close to half the first critical bending speed of the rotor.
The results of this investigation contribute to improving the design criteria of large generators installed in power plants whose exciter is often mounted on a rather long and slender end part of the shaft.

CASE STUDY

High levels of the 2X vibration of a large two-pole generator used in a combined-cycle power plant have been detected when the rotational speed reached half the first critical bending speed of the rotor. Subsequently, technical solutions to mitigate this phenomenon have been investigated.

MACHINE CONFIGURATION

Figure 1 shows a sketch of the machine layout and the identification number associated with each support. The shaft line was made by an industrial gas turbine connected to a large two-pole generator by means of a flexible load coupling. The rated power of the generator was 600 MVA. In the original configuration the generator rotor was only supported on two fixed lobe oil-film journal bearings. Each journal bearing was equipped with a pair of XY proximity probes (Figure 1) and seismic sensors that provided the measurement of the relative shaft-to-bearing vibration and the absolute vibration of the support, respectively. The nominal speed of the power unit was 3000 rpm.

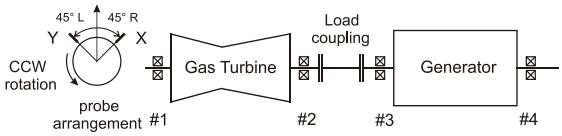


Figure 1 Sketch of the rotating machine layout considered in the study

Figure 2 shows some main geometrical characteristics of the generator rotor. The span L_2 between the two supports was 12750 mm. The slenderness index given by the ratio between the span L_2 and the average diameter of the part of the rotor contained between the two supports was 16.267. Owing to the high rated power of the generator, this slenderness index was considerable. Furthermore, the slenderness index of the overhang shaft, sited beyond the NDE support, on which the two slip rings were installed, was 5.5.

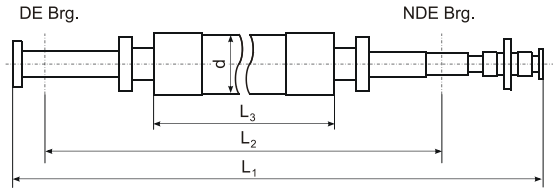


Figure 2 Sketch of the generator rotor

EXPERIMENTAL VIBRATIONS

The Bode plot of the synchronous (1X) vibrations measured in the X and Y directions, at the bearing #4 (NDE), during a machine coastdown, is illustrated in Figure 3. The passage through three critical bending speeds of the rotor is clearly pointed out by the magnification of the vibration amplitude and the corresponding change in the phase of the 1X vibration vector. The first critical speed was close to 550 rpm while the second resonance was close to 1480 rpm. A further evident resonance peak occurred at around 2720 rpm. That is, not so far from the rated speed of the power unit. The normal mode associated with this critical bending speed mainly affected the overhang shaft of the exciter, that is the end part of the rotor located beyond bearing #4. The passage through this resonance caused very high levels of the 1X vibration. This is consistent with the particular shape of the local normal mode that was quite similar to the first bending mode of a cantilever beam.

https://doi.org/10.37965/jdmd.2026.1596

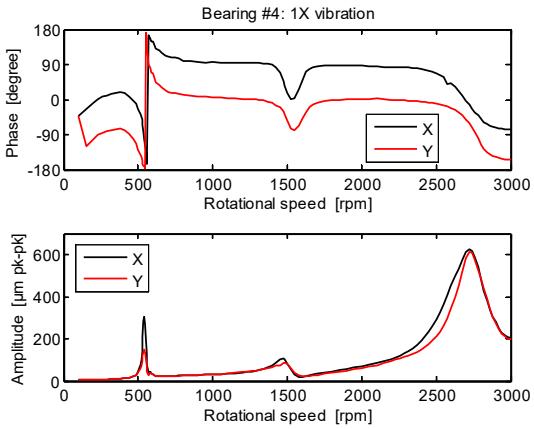


Figure 3 Bode plot of the 1X transient vibrations measured at bearing #4

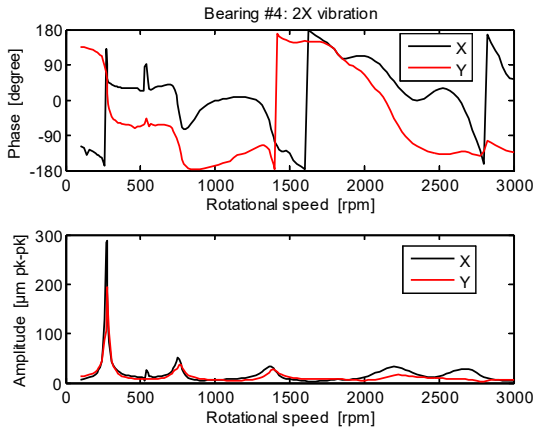


Figure 4 Bode plot of the 2X transient vibrations measured at bearing #4

Figure 4 shows the Bode plot of the 2X vibrations measured in the X and Y directions, at the bearing #4, during the same coastdown. When the rotational speed approached 270 rpm, that is half the first critical bending speed of the generator, the amplitude of the 2X vibration was subjected by a noticeable magnification and reached 290 µm pk-pk. The sharpness of this resonance peak and the corresponding fast change in the phase of the 2X vibration indicate that in this range of the rotational speed the response of the generator was lightly damped [11].

This is consistent with the common damping properties of oil-film journal bearings at very low rotational speeds. Although these noticeable vibration levels only occurred for very short time intervals during the speed transients, they might cause important fatigue stress in some critical parts of the rotor and the risk of rubs between the tip of the blades of the generator fans and stationary parts. It should also be noted that when the rotational speed was close to 270 rpm the excitation of the first bending mode of the shaft certainly caused vibration levels at the middle of the active part of the generator that were significantly higher than those measured at the journal bearings. Unfortunately, these vibrations cannot be measured.

Figure 4 points out that further very minor peaks of the amplitude of the 2X vibration also occurred at rotational speeds whose value is half the other critical bending speeds of the rotor. Anyhow they confirmed the values of the shaft critical speeds highlighted by the synchronous response of the generator.

MATHEMATICAL MODEL

Figure 5 shows the cross-section of the active part of the generator. The large number of radial slots housing the copper bars and the two poles of the generator cause different values of the two area moments of inertia of the cross-section evaluated about the principal axes. These area moments of inertia have been evaluated with a classical numerical approach implemented in an in-house code developed by the authors. In the present case study, the ratio between these area moments of inertia was 0.697.

To reproduce the 2X vibration induced by the anisotropy of the active part of the machine, a dedicated mathematical model of the generator was developed [12]. The rotor is discretized in the finite element model shown in Figure 6 using beam elements, each having constant outer and inner diameters [13]. This model also accounts for the mechanical characteristics of the oil-film journal bearings and of the supporting structure [14], [15].

https://doi.org/10.37965/jdmd.2026.1596

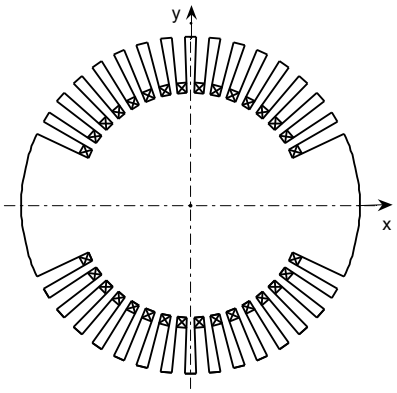


Figure 5 Cross-section of the active part of the generator rotor

Values of the stiffness and damping coefficients of the two-lobe journal bearings [16], which depend on the shaft rotational speed [17], were supplied by the bearing manufacturer.

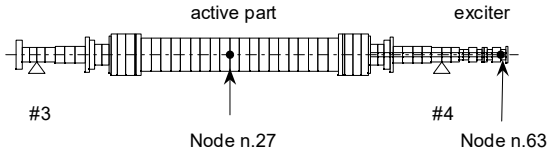


Figure 6 Finite element model of the generator rotor

The intermediate shaft that connects the generator to the gas turbine ensured a satisfactory dynamic uncoupling between the two machines. Therefore, it is possible to assume that the 2X vibrations of the generator are weakly affected by the dynamic behavior of the gas turbine. Then, the investigation on the 2X vibration has been performed only considering the generator rotor. Furthermore, in the range of rotational speeds below 900 rpm it is possible to assume that the dynamic effects of the residual imbalance of the shaft only cause a minor contribution to the 2X vibration of the shaft. On the contrary, they mainly depend on the effects of the machine weight and the periodic variations of the vertical bending stiffness of the shaft induced by the anisotropy of the active part of the generator rotor.

The equations of motion of the rotor system can be expressed as [18], [19]:

$$\left[\mathrm{M}(\vartheta)\right]\ddot{\mathrm{x}} + \left(\left[\mathrm{C}(\vartheta,\Omega)\right] + \Omega\left[\mathrm{G}(\vartheta)\right]\right)\dot{\mathrm{x}} + \\ + \left[\mathrm{K}(\vartheta,\Omega)\right]\mathrm{x} = \left[\mathrm{W}\right] + \mathrm{F}(t) \quad (1)$$

where $\left[\mathrm{M}\right]$ is the global mass matrix, $\left[\mathrm{C}\right]$ is the global damping matrix, $\left[\mathrm{G}\right]$ is the gyroscopic matrix, $\left[\mathrm{K}\right]$ is the global stiffness matrix. Due to the anisotropy of the active part of the generator some terms of these matrices depend on the shaft rotation, ϑ. The matrix $\left[\mathrm{W}\right]$ refers to the weight of the rotating parts and the supporting structure. The stiffness matrix $\left[\mathrm{K}\right]$ and the damping matrix $\left[\mathrm{C}\right]$ contain the stiffness and damping coefficients of the oil-film journal bearings that depend on the shaft angular velocity Ω. The vector $\mathrm{F}(t)$ represents the exciting forces that reproduce the dynamic effects of the residual shaft imbalance. The vector $\mathrm{x}(t)$ collects the translational and rotational displacements of the rotor system.

An eigenvalue analysis of the model was carried out to determine the theoretical critical bending speeds of the generator (Table 1). The results of this study agree well with those obtained from the analysis of the experimental vibration data, confirming that the model reproduces the actual dynamic behavior of the generator with adequate accuracy.

Table 1 Critical bending speeds

CRITICAL BENDING SPEEDS		
EXPERIMENTAL	THEORETICAL	NORMAL MODE
540 rpm	540 rpm	1st bending mode
1475 rpm	1499 rpm	2nd bending mode
2720 rpm	2715 rpm	1st bending mode of the overhang shaft

Furthermore, an eigenmode analysis was performed to evaluate the shape of the first three bending normal modes of the rotor. Figure 7 shows the shape of the first bending mode associated with the critical speed of 540 rpm. The excitation of this normal mode also causes important lateral vibrations of the overhang shaft where the slip rings of the exciter are installed. In accordance with the typical shape of the first bending mode of a shaft mounted on two supports the highest vibration amplitude occurs near the midspan between the two journal bearings.

https://doi.org/10.37965/jdmd.2026.1596

The mode shape of the eigenmode associated with the critical bending speed of 2715 rpm is shown in Figure 8. This is a local bending mode that mainly affects the overhang shaft of the exciter. At the rated speed the dynamic behavior of the end part of the generator rotor was affected by the effects of this resonance. Even in case of a satisfactory residual imbalance of the shaft the 1X lateral vibration both at the free end of the generator and at the slip rings could be rather high. This was confirmed by the vibration measurements.

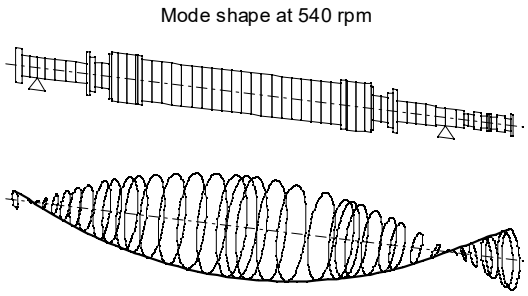


Figure 7 Shape of the 1st normal mode

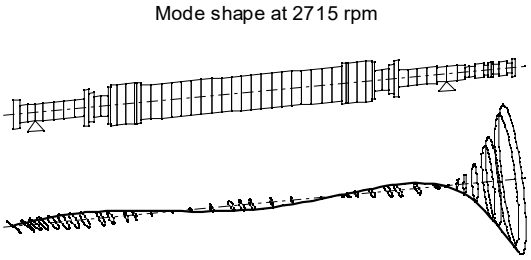


Figure 8 Shape of the 3rd normal mode

Then, the numerical model of the rotor system has been used to estimate the generator's response in the rotational speed range up to 900 rpm. The equations of motion of the system have been integrated in the time domain considering constant rotational speeds spaced each other by 1.25 rpm. For each rotational speed the integration time-step has been chosen to be an integer submultiple of the rotational period of the shaft. This way the harmonic orders of the system vibration obtained with the model have been evaluated with good accuracy avoiding any possible leakage error.

For each case study the integration of the equations of motion has been stopped after checking for a satisfactory convergence of the results. These results have been used as initial conditions of motion for the analysis of the system response at the subsequent rotational speed.

The principal axes of inertia of the cross-sections of the active part of the generator rotor coincide with the horizontal and vertical axes shown in Figure 5. The angular position of these axes is fixed with the shaft. Therefore, during a full revolution of the generator the orientation of the principal axes of inertia changs with respect to the horizontal and vertical axes of the Cartesian reference frame of the finite element model of the rotor used to evaluate the dynamic behavior of the system.

Owing to this, the orientation of the principal axes of inertia of the beam finite elements used to model the active part of the generator rotor has been varied at any time-step of the integration process of the differential equations of motion depending on the corresponding angular position of the shaft. Owing to the periodic variations of the horizontal and vertical bending stiffness of the main body of the generator rotor that occur during a full revolution of the shaft line 2X lateral vibrations are generated. The complex bending of the shaft causes vibrations both in vertical and horizontal direction.

Figure 9 shows the periodic variations in the area moments of inertia of the cross-sections of tha active part of the generator evaluated with respect to the horizontal and vertical axes of the Cartesian reference frame of the finite-element model of the rotor during a full revolution. Figure 10 shows the corresponding variations of the product of inertia of area evaluated during a full revolution of the shaft.

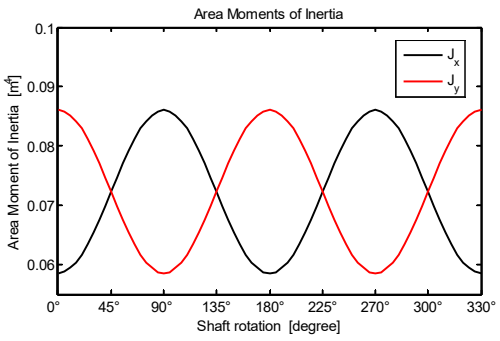


Figure 9 Variations of the area moments of inertia evaluated with respect to the horizontal and vertical axes during a full revolution of the shaft

https://doi.org/10.37965/jdmd.2026.1596

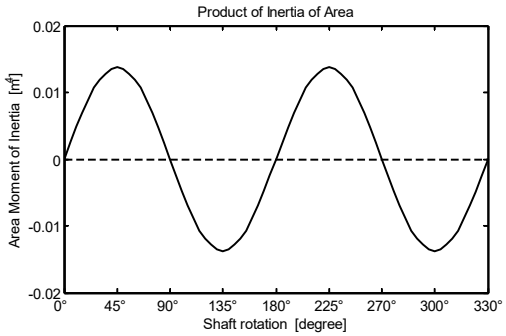


Figure 10 Variations of the product of inertia of area evaluated during a full revolution of the shaft

An arbitrary set of local imbalances, which have been applied to the model of the generator, has been determined in order to obtain 1X vibrations, evaluated at the journal bearings, which were in satisfactory accordance with the related experimental findings at least in the rotational speed range up to 900 rpm. These local imbalances have been estimated with an identification method, developed by the authors in the past, based on the minimization of the error between the numerical response and the corresponding 1X experimental vibrations measured during speed transients [21, 22].
More in particular, Figure 6 shows the axial position of the two local imbalances that have been applied at nodes 27 and 63 of the finite element model. Magnitude and angular position of these two equivalent imbalances are shown in Table 2.

Table 2 Equivalent local imbalances

	IMBALANCE	
NODE	MAGNITUDE	PHASE
27	0.4250 kgm	0°
63	0.0120 kgm	0°

Figure 11 shows the Bode-plot of the theoretical 1X vibration induced at the NDE bearing of the generator, in the X and Y directions, by the local imbalances mentioned above. The comparison between the experimental 1X vibration shown in Figure 3 and corresponding numerical results shown in Figure 11 proves that in the passage through the first critical speed of the shaft the set of the equivalent local imbalances causes synchronous vibrations that are quite similar to the experimental ones. These results strengthened the belief that the model was sufficiently accurate and that also the 2X vibrations could be properly estimated.

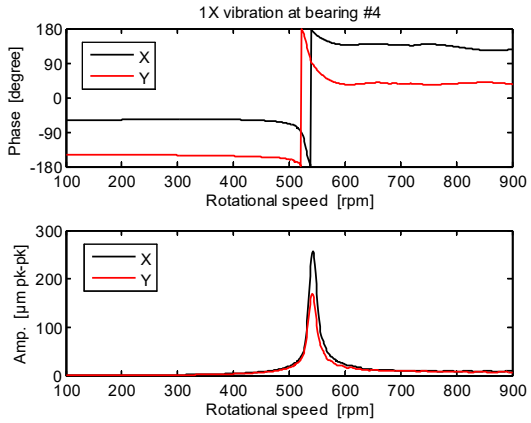


Figure 11 Bode plot of the theoretical 1X vibration evaluated at bearing #4

The goal of this investigation, based on the integration of the equations of motion of the system in the time domain, was to simulate the 2X vibration of the generator. When the rotational speed is not very high this super-synchronous harmonic component of the system response is weakly influenced by the synchronous excitations.
Figure 12 shows the Bode plot of the theoretical 2X vibration induced at the NDE bearing of the generator in the speed range up to 900 rpm. The curves of the amplitude of this vibration show an evident peak at a rotational speed very close to 270 rpm. The peak level of this 2X vibration is close to 300 µm pk-pk.
When the rotational speed approaches half the first critical bending speed of the generator the curves of the phase of the 2X vibration vectors show an evident change. This behavior is in good accordance with the experimental findings (Figure 4).

https://doi.org/10.37965/jdmd.2026.1596

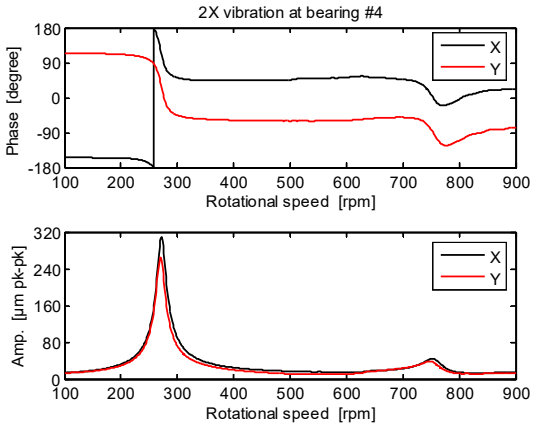


Figure 12 Bode plot of theoretical 2X vibration evaluated at bearing #4

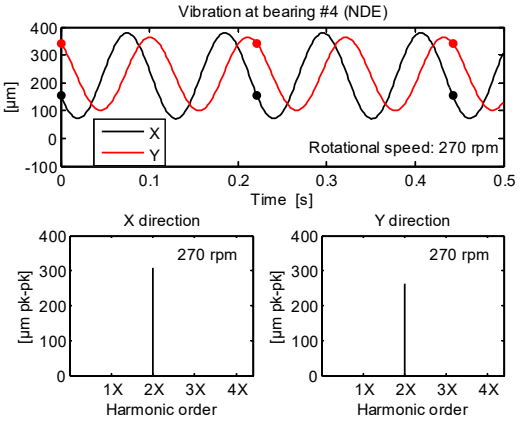


Figure 13 Numerical results obtained for a rotational speed of 270 rpm

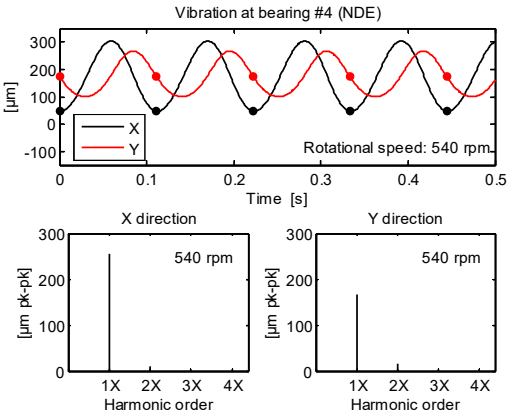


Figure 14 Numerical results obtained for a rotational speed of 540 rpm

A further minor peak of the amplitude of the theoretical 2X vibration provided by the model is quite detectable in the speed range close to 740 rpm. The corresponding change in the curves of the phase of this harmonic component confirms the presence of a further critical speed of the model at around 1480 rpm. These numerical results are also consistent with the behavior indicated by the monitoring data.

The theoretical 2X vibrations obtained with the model demonstrate that the dynamic effects caused by the weight loading and the periodic variations of the bending stiffness of the shaft can be successfully simulated with the investigation method used by the authors.

Figure 13 shows a short portion of the timewave of the theoretical vibrations evaluated with the model at the NDE bearing, in the X and Y directions, at a rotating speed of 270 rpm. The frequency spectrum of these vibrations is shown in the lower part of the same figure. The timewave of the theoretical vibration is dominated by the 2X harmonic component while the amplitude of the 1X harmonic order is negligible. These results are in accordance with the experimental findings shown in Figures 3 and 4. Similarly, Figure 14 shows a short portion of the timewave of the theoretical vibration evaluated at a rotating speed of 540 rpm. The corresponding frequency spectrum is dominated by the synchronous harmonic component.

The Bode plots illustrated in Figures 15 and 16 show a comparison between the 2X experimental vibrations and the corresponding numerical response evaluated at the NDE bearing of the generator, in the X and Y directions, respectively, within the rotational speed range up to 900 rpm. The correspondence between numerical results and experimental data is rather good both for the amplitude and the phase of the 2X vibration vectors.

https://doi.org/10.37965/jdmd.2026.1596

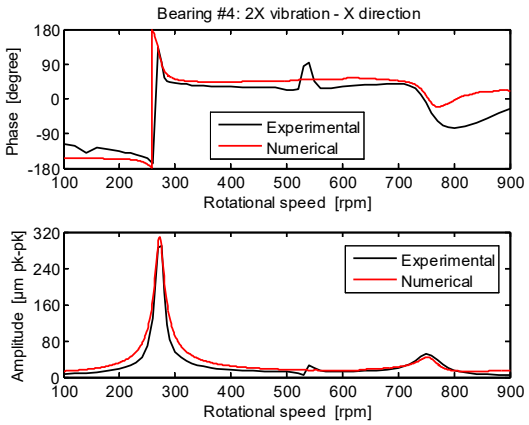


Figure 15 Comparison between experimental and theoretical 2X vibration evaluated at bearing #4 in the X direction

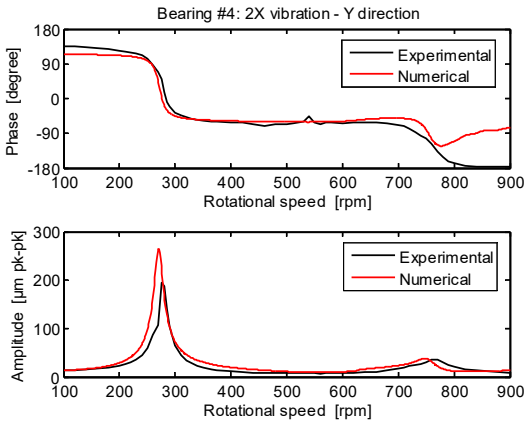


Figure 16 Comparison between experimental data and theoretical 2X vibration evaluated at bearing #4 in the Y direction

Figure 17 shows a comparison between the 2X filtered orbits obtained at 270 rpm by comparing monitoring data against numerical results. The effect of the weight loading and the periodic variations of the bending stiffness of the active part of the rotor causes 2X elliptical orbits whose main principal axis in almost oriented in vertical direction.

The results calculated with the finite element model of the generator, integrating the equations of motion in the time domain, have been processed to evaluate the dynamic deflection of the rotor at some rotational speeds of interest. The shape of the dynamic deflection of the generator evaluated at 270 rpm, which also includes the sag due to gravity, is illustrated in Figure 18. At this rotational speed the whirl orbits, plotted at a limited number of cross-sections of the shaft, in order to make the figure more readable, are almost elliptical being dominated by the 2X harmonic component of the lateral vibration.

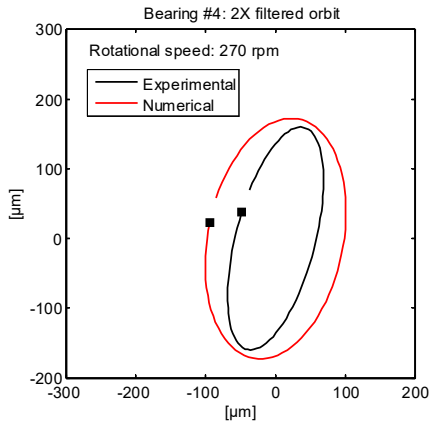


Figure 17 2X filtered orbits evaluated at 270 rpm: comparison between experimental data and numerical results

The plain curve connects the point of each orbit evaluated at a given time instant. This curve relates to the dynamic deflection of the shaft. At any cross-section the whirling motion of the rotor occurs around the dotted line that is shown in the same figure. Since the rotor weight and the periodic variations of the vertical bending stiffness of the shaft excite the first balance resonance of the generator the maximum vibration amplitude occurs near the midspan between the two supports (2730 µm pk-pk). However, the overhang shaft of the exciter is also affected by an important deflection and considerable vibration levels. Figure 19 shows the dynamic deflection of the generator evaluated at 540 rpm. That is, at the first critical bending speed of the rotor.

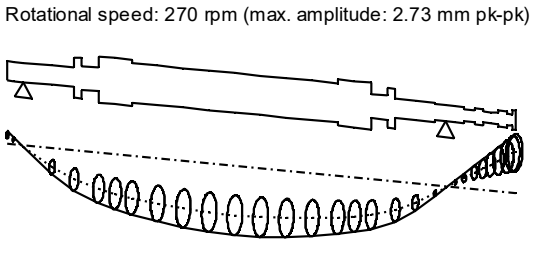


Figure 18 Shaft dynamic deflection evaluated at 270 rpm

https://doi.org/10.37965/jdmd.2026.1596

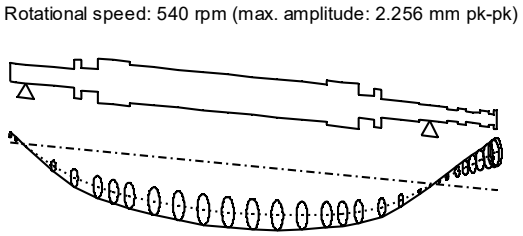


Figure 19 Shaft dynamic deflection evaluated at 540 rpm

Again, the dynamic deflection includes the sag due to gravity. Therefore, the shape of this dynamic deflection of the shaft is quite similar to that which occurs at 270 rpm. However, in this case the whirling orbits are mainly affected by the 1X-harmonics of the shaft vibration.

During the performance tests of this power unit very high 1X vibrations were detected at the NDE journal bearing both at the operating speed and in the speed range around 2700 rpm. This dynamic behavior was caused by the excitation of the local normal mode of the overhang shaft of the exciter associated with a critical speed of 2720 rpm (Table 1).

Based on the shape of the normal mode shown in Figure 8 it was suspected that the 1X vibration levels that occurred at 3000 rpm downstream of the exciter were considerable. Therefore, a laser probe was installed at the free end of the generator. Figure 20 shows the Bode plot of the 1X and 2X vibrations measured during a speed transient with this probe.

The amplitude of the 1X vibrations measured at rotational speed values above 2500 rpm was approximately ten times higher than that measured at bearing #4, reaching a peak level of 5540 μm pk-pk. This is in accordance with the shape of the normal mode illustrated in Figure 8.

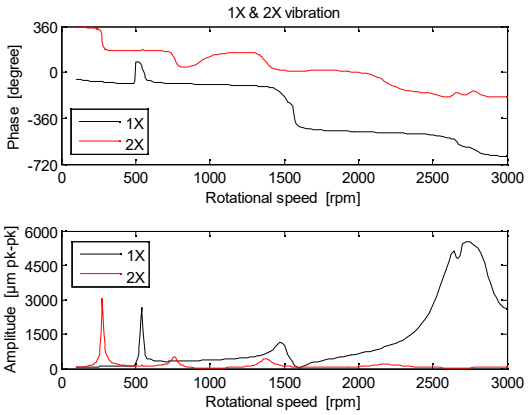


Figure 20 Bode plot of the 1X and 2X transient vibrations measured at the free end of the generator

GENERATOR MOUNTED ON THREE SUPPORTS

The vibration data collected at 3000 rpm at both Full-Speed-No-Load (FSNL) and base load operating condition, with the generator rotor supported on two main journal bearings, indicated that the overhang shaft of the exciter was frequently subjected to significant levels of the lateral vibration. In order to ensure safety operating conditions and reduce the rate of wear of the carbon brushes that are in contact with the slip rings it was decided to install an additional journal bearing at the end of the overhang shaft of the exciter.

This change in the original design of the generator required to connect a short stub shaft to the free end of the overhang shaft of the exciter. This stub shaft was only 500 mm long while its diameter was 200 mm. A flange located at the drive end side of the stub shaft and a further flange mounted on the free end of the generator rotor made it possible to connect the two shafts each other. Then, an additional pedestal was fixed to the concrete foundation of the power unit and a five-shoe tilting-pad journal bearing was installed inside this additional support [20], located at the free end of the stub shaft.

The main goal of this partial but fundamental modification of the original design of the generator rotor was to cause a significant increase above 3000 rpm of the critical bending speed whose original value was close to 2720 rpm. In addition, it was it was foreseeable that this modification would cause an important change in the shape of the dynamic

https://doi.org/10.37965/jdmd.2026.1596

deflection of the end part of the shaft where the slip rings were located.

At the end of the modifications carried out on the system the power unit was started up and operated up to the base load. The Bode plot of the synchronous (1X) vibrations measured in the X and Y directions, at the bearing #4 (NDE), during a machine speed transient is illustrated in Figure 21. These 1X vibrations can be compared to those shown in Figure 3, when the rotor was only mounted on two supports. It is quite evident that the installation of the additional journal bearing at the end of the shaft of the exciter has shifted up beyond 3000 rpm the critical bending speed that originally occurred at 2720 rpm. As a result, the amplitude of the 1X vibration measured at 3000 rpm at bearing #4 and at the end of the exciter shaft decreased significantly. In addition, the installation of the additional support also caused a partial increase of the first critical bending speed from 540 rpm to 600 rpm.

The Bode plot of the 2X vibrations measured in the X and Y directions, at the bearing #4 (NDE), during the same speed transient is shown in Figure 22. When the rotational speed approached 300 rpm the 2X vibration amplitude increased up to a peak value of 70 µm pk-pk. This amplitude is four times lower than the peak level that occurred when the only two journal bearings supported the generator (Figure 4). This dynamic behavior proved to be repeatable during every further speed transient. As a result, the installation of the additional support at the end of the shaft of the exciter has caused a considerable mitigation of the peak level of the 2X vibration when the rotating speed reaches half the first critical bending speed of the generator rotor.

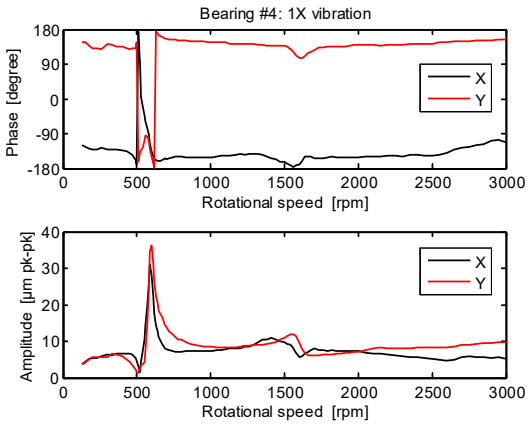


Figure 21 Bode plot of the 1X transient vibrations measured at bearing #4

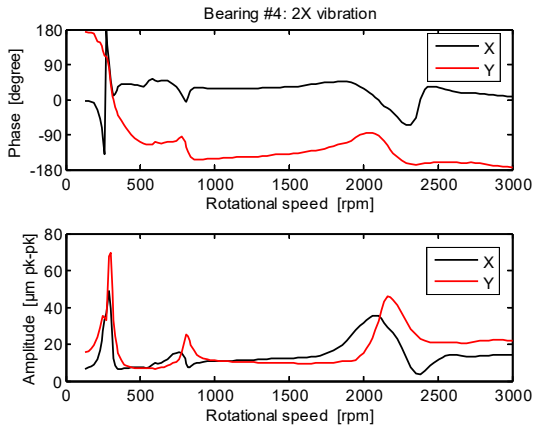


Figure 22 Bode plot of the 2X transient vibrations measured at bearing #4

The Bode plot of the 1X vibrations measured in the X and Y directions at the additional bearing #5 is shown in Figure 23. It is possible to note that the amplitude of these vibrations, measured downstream of the exciter, were significantly lower than those measured with the laser probe, almost at the same cross-section, when the generator was mounted on only two bearings (Figure 20).

This beneficial effect generated in the dynamic behavior of the overhang shaft of the exciter was due to the installation of the additional bearing.

The Bode plot of the 2X vibrations measured in the X and Y directions, at the additional bearing #5, is shown in Figure 24. A peak of the 2X harmonic component at 300 rpm is also present in the vibrations measured at bearing #5. However, the amplitude of these vibrations did not exceed 100 µm pk-pk. Moreover, a further magnification of the 2X vibration level occurred in the speed range around 2200 rpm. This indicates that the installation of the additional journal bearing #5 caused a shift of the critical speed originally located at 2720 rpm to a value of approximately 4400 rpm. That is far away from the rated speed of 3000 rpm.

https://doi.org/10.37965/jdmd.2026.1596

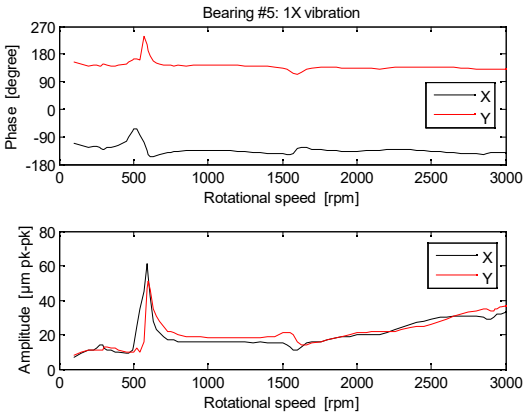


Figure 23 Bode plot of the 1X transient vibrations measured at bearing #5

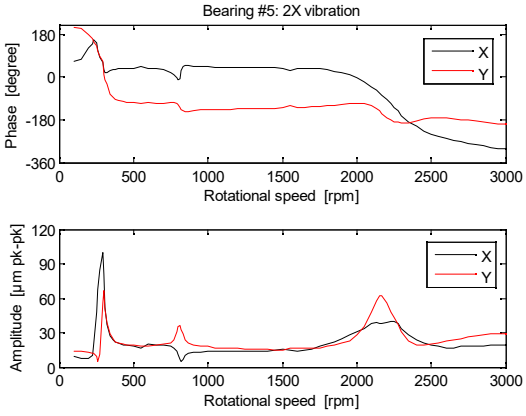


Figure 24 Bode plot of the 2X transient vibrations measured at bearing #5

The reasons for the substantial improvement in the machine dynamic behavior caused by the installation of the additional bearing were investigated using a model-based method.

Figure 25 shows the new finite element model of the generator rotor supported on three journal bearings.

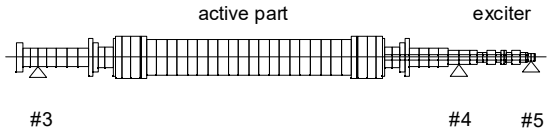


Figure 25 Finite-element model of the generator rotor supported by three journal bearings

The same local imbalances used for the previous analysis have been applied to the model (Table 2).

Then, the behavior of the rotor system has been evaluated in the speed range up to 900 rpm by integrating the equations of motion in the time domain and applying the same investigation method described above.

Figure 26 shows the Bode-plot of the theoretical 1X vibrations induced at bearing #4 by the local imbalances. The maximum amplitude of the 1X vibration evaluated at the first critical bending speed is 44 µm pk-pk. This peak level is about five times lower than that caused by the same local imbalances applied to the model of the rotor supported on only two journal bearings (Figure 11). This result is in accordance with the experimental findings.

Figure 27 shows the Bode-plot of the 2X vibrations evaluated at bearing #4. The peak level of this 2X vibration evaluated at about 300 rpm is 120 µm pk-pk.

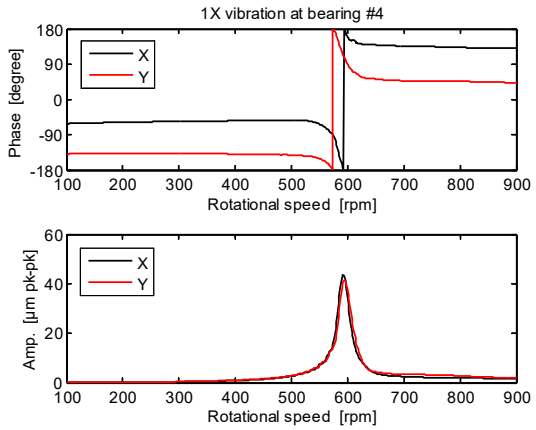


Figure 26 Bode plot of the theoretical 1X vibration evaluated at bearing #4

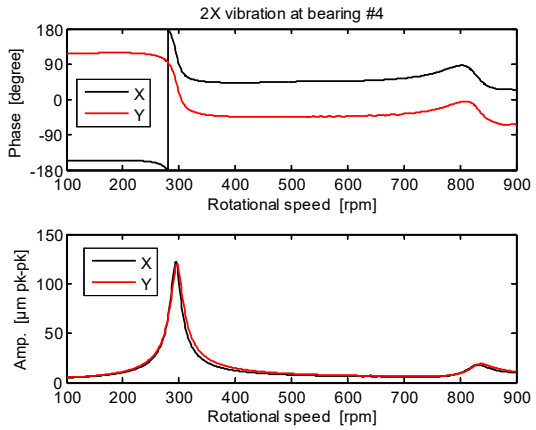


Figure 27 Bode plot of the theoretical 2X vibration evaluated at bearing #4

https://doi.org/10.37965/jdmd.2026.1596

This peak is about 2.6 times lower than that caused by the same local imbalances applied to the model of the rotor supported on only two journal bearings (Figure 12). Therefore, the numerical results also confirm that the installation of the additional bearing can cause a significant mitigation of the peak of the 2X vibration at half the first critical speed of the generator. However, the model overestimated the amplitude of this theoretical 2X vibration compared to the corresponding experimental value.

Anyhow, it is necessary to consider that the sharpness of the resonance peak is considerable and the resolution with which the theoretical response has been evaluated (1.25 rpm) is higher than that of 10 rpm with which the monitoring data were recorded during the speed transients.

Furthermore, for every rotational speed of interest, the numerical response has been evaluated in a steady-state condition while the experimental data have been collected during speed transients. Although the deceleration of the shaft line is rather low during the final part of the coastdown the slowdown rate could cause lower levels of the system response compared to the corresponding theoretical results.

Then, the results obtained integrating the equations of motion in the time domain have been processed to evaluate the dynamic deflection of the rotor at some rotational speeds of interest. The dynamic deflection of the generator evaluated at 292 rpm is illustrated in Figure 28. At this rotational speed the whirling orbits are almost elliptical, being dominated by the 2X harmonic component of the lateral vibration.

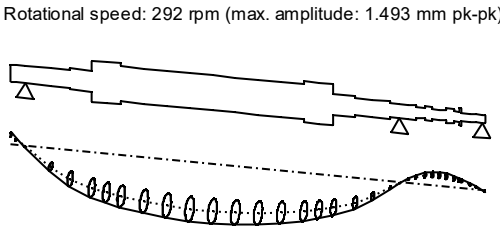


Figure 28 Shaft dynamic deflection evaluated at 292 rpm

The plain curve, which connects the point of each orbit evaluated at the same given time instant, refers to the dynamic deflection of the shaft. Since the rotor weight and the periodic changes in the vertical bending stiffness of the shaft-line excite the first natural frequency of the generator the maximum amplitude of the vibration occurs near the midspan between the two supports (1493 μm pk-pk). This amplitude, which mainly depends on the anisotropy of the shaft and the weight loading, is about 1.8 times lower than that evaluated with the generator mounted on only two supports.

Figure 29 shows the dynamic deflection of the generator evaluated at 596 rpm. That is, at the first critical bending speed of the modified rotor. Therefore, the shape of this dynamic deflection of the shaft is quite similar to that which occurs at 292 rpm. However, in this case the whirling orbits are mainly affected by the 1X harmonic component.

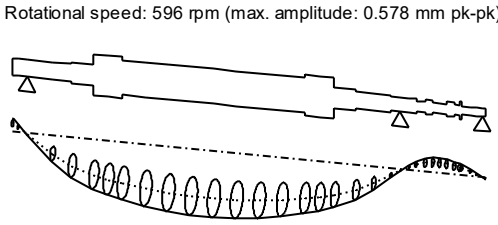


Figure 29 Shaft dynamic deflection evaluated at 596 rpm

The presence of the additional support installed at the end of the shaft of the exciter has modified the mode shape of the first normal mode, significantly, especially in the part of the rotor beyond the main NDE journal bearing. With regard to the mode shape of the first mode, the considerable change in the curvature of the dynamic deflection that occurs in the part of the shaft where the slip rings are installed causes an important mitigation of the peak amplitude of the vibrations of the active part of the generator induced by the excitation of the 2X resonance and by crossing the first bending critical speed. As a result, when the first resonance is excited the amplitude of the vibrations generated near the main journal bearings is also mitigated considerably.

A few months after the commissioning of the power unit whose vibrations have been analyzed in the present paper a further turbogas unit, composed of an identical gas turbine and generator, was installed at another power plant. In this case, based on the previous experience, the additional journal bearing downstream the exciter was installed from the outset.

To validate and confirm the beneficial effects resulting from the installation of the additional journal bearing the 2X transient vibrations measured at bearing #4 of this new power unit have been shown in Figure 30.

https://doi.org/10.37965/jdmd.2026.1596

This 2X response of the generator is rather similar to that shown in Figure 22. This demonstrates the real effectiveness of installing an additional journal bearing at the end of the overhang shaft of the exciter aimed at mitigating the amplitude of the 2X vibrations that occur when the rotational speed approaches half the first critical speed of the generator.

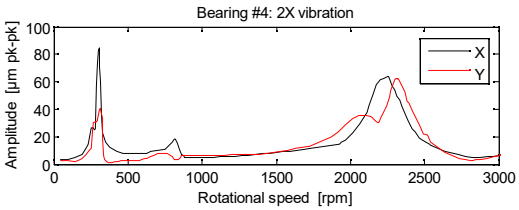


Figure 30 2X transient vibrations measured at bearing #4 in another power plant

CONCLUSION

It is well established that the anisotropy of the active part of large two-pole generators causes 2X vibrations whose amplitude depends on the machine rotational speed. The excitation of the 2X resonance that occurs when the rotating speed reaches half the first critical bending speed of the shaft may cause very high levels of the 2X vibration detected at the generator's journal bearings.

In this paper the effects of the overhang shaft of the exciter on the amplitude of the shaft vibrations connected to the 2X resonance have been investigated with a model-based method. The numerical results obtained with the model have been compared to experimental vibration data collected on a large power unit.

The results of this investigation have shown that when the overhang shaft of large two-pole generators is rather long and slim it may be very useful to install an additional journal bearing at the free end of the exciter shaft. This further constraint not only mitigates the 1X vibration levels of the slip rings when the rotating speed reaches the lowest critical bending speeds of the generator that are below the rated speed but also causes a considerable mitigation of the level of the 2X vibrations that occur at the two main journal bearings when the rotational speed gets close to half the first critical bending speed. Frequently, when large generators are only mounted on two main supports the amplitude of the 2X vibration caused by the first 2X resonance is considerable and the mechanical stress due to this phenomenon may cause the initiation of cracks at critical cross-sections of shaft line. Installing additional support at the end of the exciter shaft can significantly mitigate the risk of these issues arising. Clearly, the installation of this support also reduces the amplitude of the 1X vibration that occurs at the rated speed.

REFERENCES

[1] J. Hidalgo and A. K. Dhingra, 'High-Speed Balancing of Rotors with Overhangs: When Is Overhang Likely to Cause Problems?', J. Test. Eval., 2006, doi: 10.1520/JTE12628.

[2] R. Viitala, T. Tiainen, and R. Viitala, 'Effect of Rotor Geometry on Bending Stiffness Variation', Machines, vol. 9, no. 2, p. 23, 2021, doi: 10.3390/machines9020023.

[3] M. Sakata, M. Endo, K. Kishimoto, and N. Hayashi, 'Secondary critical speed of flexible rotors with inertia slots', J. Sound Vib., vol. 87, no. 1, pp. 61–70, 1983, doi: 10.1016/0022-460X(83)90439-X.

[4] S. Huang, Z. Liu, and J. Su, 'On Double Frequency Vibration of a Generator-Bearing System With Asymmetrical Stiffness', in Proceedings of IMECE2002, ASME International Mechanical Engineering Congress & Exposition, New Orleans, LA, USA, Nov. 2002. doi: 10.1115/IMECE2002-39229.

[5] Z. Zheng, Y. Xie, and D. Zhang, 'Numerical Investigation on the Gravity Response of a Two-Pole Generator Rotor System with Interval Uncertainties', Appl. Sci., vol. 9, no. 15, p. 3036, 2019, doi: 10.3390/app9153036.

[6] C. H. Park, Y. C. Kim, K. G. Cho, and B. S. Yang, 'Prediction of 2X Vibration of a Generator Rotor with Asymmetric Shaft Stiffness', J. Power Syst. Eng., vol. 11, no. 1, 2007.

[7] J. P. Park, 'Diagnosis of excessive vibration signals of two-pole generator rotors in balancing', KSME Int. J., vol. 14, pp. 590–596, 2000, doi: 10.1007/BF03184435.

https://doi.org/10.37965/jdmd.2026.1596

[8] ISO, ‘Mechanical Vibration — Evaluation of Machine Vibration by Measurements on Rotating Shafts — Part 3: Coupled Industrial Machines’, International Organization for Standardization, Geneva, Switzerland, ISO 7919-3:2009, 2009.

[9] A. Chasalevris, I. Gavalas, and J. Sawicki, ‘Optimal bearing configuration selection for power generation shaft-trains: A linear and nonlinear dynamics approach’, J. Sound Vib., vol. 559, p. 118907, 2024, doi: 10.1016/j.jsv.2024.118907.

[10] N. Bachschmid, P. Pennacchi, and E. Tanzi, Cracked Rotors: A Survey on Static and Dynamic Behaviour Including Modelling and Diagnosis. Berlin, Germany: Springer, 2010. doi: 10.1007/978-3-642-01485-7.

[11] L. N. Virgin, ‘Interrogating the Lead-Up to a Critical Speed in Rotordynamics’, J. Vib. Acoust., vol. 144, no. 3, p. 031012, 2022, doi: 10.1115/1.4053190.

[12] D. Childs, Turbomachinery Rotordynamics: Phenomena, Modeling, and Analysis. New York, NY, USA: John Wiley & Sons, 1993.

[13] G. Genta, Dynamics of Rotating Systems. New York, NY, USA: Springer, 2005.

[14] M. Adams, Rotating Machinery Vibration. New York, NY, USA: Marcel Dekker, 2001.

[15] M. Hajžman, M. Balda, P. Polcar, and P. Polach, ‘Turbine Rotor Dynamics Models Considering Foundation and Stator Effects’, Machines, vol. 10, no. 2, p. 77, 2022, doi: 10.3390/machines10020077.

[16] T. Someya, Ed., Journal-Bearing Databook. Berlin, Germany: Springer, 1989.

[17] G. B. Benti, R. Gustavsson, and J.-O. Aidanpää, ‘Speed-Dependent Bearing Models for Dynamic Simulations of Vertical Rotors’, Machines, vol. 10, no. 7, p. 556, 2022, doi: 10.3390/machines10070556.

[18] M. Lalanne and G. Ferraris, Rotordynamics Predictions in Engineering. Chichester, UK: John Wiley & Sons, 1998.

[19] A. Muszynska, Rotordynamics. New York, NY, USA: CRC Taylor & Francis, 2005.

[20] J. C. Wilkes and D. W. Childs, ‘Tilting Pad Journal Bearings — A Discussion on Stability Calculation, Frequency Dependence, and Pad and Pivot Flexibility’, J. Eng. Gas Turbines Power, vol. 134, no. 12, p. 122508, 2012.

[21] P. Pennacchi, N. Bachschmid, A. Vania, G. A. Zanetta, L. Gregori, 'Use of modal representation for the supporting structure in model-based fault identification of large rotating machinery: part 1 - theoretical remarks', MSSP Journal, vol. 20, 2006, pp. 662-681, doi: 10.1016/j.ymssp.2004.11.006.

[22] P. Pennacchi, A. Vania, N. Bachschmid, 'Increasing the robustness of fault identification in rotor dynamics by means of M-estimators’, MSSP Journal, vol. 21, 2007, pp. 3003-3029, doi: 10.10.1016/j.ymssp.2007.04.001.